Hindawi Publishing Corporation
Mathematical Problems in Engineering
Volume 2016, Article ID 5682847, 13 pages
http://dx.doi.org/10.1155/2016/5682847

Research Article

Wavelet-Based Feature Extraction in Fault Diagnosis for Biquad High-Pass Filter Circuit

Yuehai Wang,[1] Yongzheng Yan,[1] and Qinyong Wang[2]

[1]*School of Electrical Information and Engineering, North China University of Technology, Beijing 100144, China*
[2]*Technical Support and Service Center, Beijing Open University, Beijing 100081, China*

Correspondence should be addressed to Yuehai Wang; wangyuehai@ncut.edu.cn

Received 21 March 2016; Revised 5 July 2016; Accepted 8 August 2016

Academic Editor: Paolo Crippa

Fault diagnosis for analog circuit has become a prominent factor in improving the reliability of integrated circuit due to its irreplaceability in modern integrated circuits. In fact fault diagnosis based on intelligent algorithms has become a popular research topic as efficient feature extraction and selection are a critical and intricate task in analog fault diagnosis. Further, it is extremely important to propose some general guidelines for the optimal feature extraction and selection. In this paper, based on wavelet analysis, we will study the problems of mother wavelets selection, number of decomposition levels, and candidate coefficients selection by using a four-op-amp biquad filter circuit. After conducting several comparative experiments, some general guidelines for feature extraction for this type of analog circuits fault diagnosis are derived.

1. Introduction

Due to development of modern integrated circuit technology, many new electronic circuits have been created not only with greater complexity but also with basic circuit elements being inaccessibly embedded within circuit chips. Therefore fault detection and diagnostic techniques have been of interest to many researchers in circuits and systems, especially in system reliabilities. Despite the dominant role of digital and microprocessor in modern integrated circuits, analog circuits are very important in many electronic devices [1, 2]. In fact, although large electronic systems are usually implemented by digital techniques, quite often they interface with external world through analog devices such as sensors for inputs, AD/DA converters for signal processing, and actuators for outputs [3]. In consequence, the diagnosis of analog circuits in a mixed analog-digital system is indispensable for many applications. The objective of analog circuit fault diagnosis is to determine the fault types, components, and parameters once the abnormal circuit response is detected when we know the topology of circuit, stimulus signal, and response data of the circuit. The fault diagnosis, with the network analysis and network synthesis, is considered to be one of the three branches of modern circuit theory [4]. Berkowitz [5] in 1962 found the first general necessary condition for network-element-value solvability, and then Navid and Willson [6] in 1979 presented some sufficient conditions for resistive network by component simulation, which established the general theoretical foundation for the study of analog circuit fault diagnosis. In the 1970s, a considerable amount of researches has been focused on the techniques about fault dictionary method, the testability of the circuits, components fault diagnosis, and multiple fault diagnosis. In 1985, Bandler and Salama [7] addressed the theory and algorithms associated with various fault location techniques in analog networks. In recent years, the intelligent diagnosing approaches based on various pattern recognition (PR) techniques have attracted much attention and a number of promising developments have emerged.

Although the fault diagnosis of analog circuit has attracted considerable attention during the past fifty years, the research in analog circuit detection and diagnosis is still considered as an extremely difficult problem [7] and has several critical issues due to the following characteristics of analog circuits: the nonlinear nature of the problem, the lack of good fault models, inaccurate analog components tolerance, difficulty and inaccuracy of the measurement, experience-dependent heuristic feature extraction, and incomplete

diagnostic knowledge. Therefore, the diagnosis for analog circuits still relies heavily on the engineer's experience and intuition and remains to be an iterative and time-consuming process. As a result, there are urgent needs to find intelligent diagnosis approaches for analog circuits and analog/digital hybrid circuits.

PR-based classifying algorithms aim to learn the diagnostic knowledge before they were used to detect and diagnose circuit faults. The diagnostic knowledge was learned from large amount of response data including normal and faulty state responses through some well-designed training procedure. When the training procedure is designed properly, a classifying algorithm can be used to detect the circuit fault type via sampling the state data, constructing the fault features, and feeding selected features to a well-designed classifier, and then obtaining the diagnostic result. An obvious advantage of such classifying algorithms is that no mathematical model of the process or comprehensive examination of circuit under test (CUT) is required. However, the success in achieving these goals is severely limited when the diagnostic knowledge captured from the sampling data lacks sufficient precision. A well-trained diagnosis approach was based not only on an appropriate classification algorithm, but also on the large amount of training data that should cover every fault class as well as effective feature extracting process that is used to select the fault features. In the past decades, some effective classifiers based on genetic algorithms [8, 9], artificial neural network [3, 10–15], wavelet theory [9, 11, 13], fuzzy theory [3, 16], artificial immune system [17–19], support vector machine [9], particle filtering [20], and clonal selection algorithm [21] were widely reported, but there were just few researches about how to extract the fault feature from responses of circuits. In fact, it is a critical procedure and primary task for general-purpose PR-based diagnosis algorithms to find some effective methods and circuit-dependent fault feature extraction and construction approaches to reduce the dimension of input data and minimize its training and processing time.

Some researchers have used various fault information content as a measure to extract the fault features, such as information cost function [22], sensitivity of characteristic parameter [23], feature departure degree [24], and principle based on minimum redundancy maximum relevance [25]. These approaches, however, usually require various types of faults posterior probability distribution functions and the density functions of observed values, which are usually hard to obtain. Some other researchers try to extract optimal feature based on the kernel function [26], but these kernel-based methods often take expensive computational costs when kernel matrix is calculated to analyze the features.

Feature extraction using wavelet analysis is a popular approach in the domain of analog circuit fault diagnosis due to the perfect local property of wavelet in both time and frequency space, which makes it an appealing approach to process noisy and unstable signals, such as transient response of analog circuit [10, 13]. But till now, there are no effective theoretical guidelines on how to choose proper wavelet functions in the field of analog circuit fault diagnosis. On the contrary, this issue is mostly based on engineers' experience or some experiments. For example, Spina and Upadhyaya in their pioneering work [10] directly used the collected samples as the input and obtained a high-dimension classifier. Aminian et al. [11, 12] used the approximation coefficient as the features and discarded the detail parts as noise to reduce the number of input features; Wang et al. [27], however, have chosen the high frequency bands to extract features since they believe that the fault information of a circuit always exists in the high frequency bands of the output signal. The defect of retaining only one part of coefficients may lead to the loss of valid information, thus with high probability of ambiguity cases and low diagnosis ability. Although many researchers [11, 13, 15, 21, 28, 29] used both low frequency approximation and detail coefficient from wavelet decomposition to construct the optimal feature factors, different processes were employed without convincing reasons. For instance, Li et al. [15, 29] selected Haar as mother wavelet and calculated the fault feature from the coefficients associated with level 3 Haar wavelet packet analysis. There are also other features reported in the existing literature, such as kurtosis and entropy [14], which were used to represent fault feature. Therefore, how to choose wavelet mother function, wavelet coefficients, and wavelet decomposition depth are still critical issues in this area [30].

In order to solve this problem, we would use a four-op-amp biquad high-pass filter [10–13, 28] as benchmark CUT. This type of analog circuit is very common in existing equipment and also is well studied in [10–13] due to its importance. Another aim for selecting this analog circuit is that we can compare the performance with previous investigations. With this four-op-amp biquad high-pass filter, we input a single impulse of height 5 V and duration of 10 μs and observe its responses. As to parametric faults, we follow the category description in [12] including mounting of components with values out of tolerance on this biquad high-pass filter, which can be used as audio frequency filter. We first compare five frequently used wavelet mother functions to solve the problem for mother wavelet selection. Then we use the selected best wavelet as preprocessor to extract the fault features hidden in circuit state data which are generated by simulation software. Finally, different feature construction methods are compared based on decomposition level and wavelet coefficients selection in terms of the diagnosis rate on the same CUT by using a Clone Selection Classification Algorithm (CSCA). Based on these investigations, we can summarize a systematic procedure on the optimal fault feature construction method in this type of analog circuit fault diagnosis, when wavelet analysis is adopted.

This paper is organized as follows. In Section 2, we will describe the framework and diagnosis procedures for intelligent diagnosis approaches based on various pattern recognition algorithms, and then we discuss the fault feature construction method on the basis of wavelet analysis in Section 3. After that, extensive comparative experiment studies are presented in Section 4. Finally, the conclusions are given in Section 5.

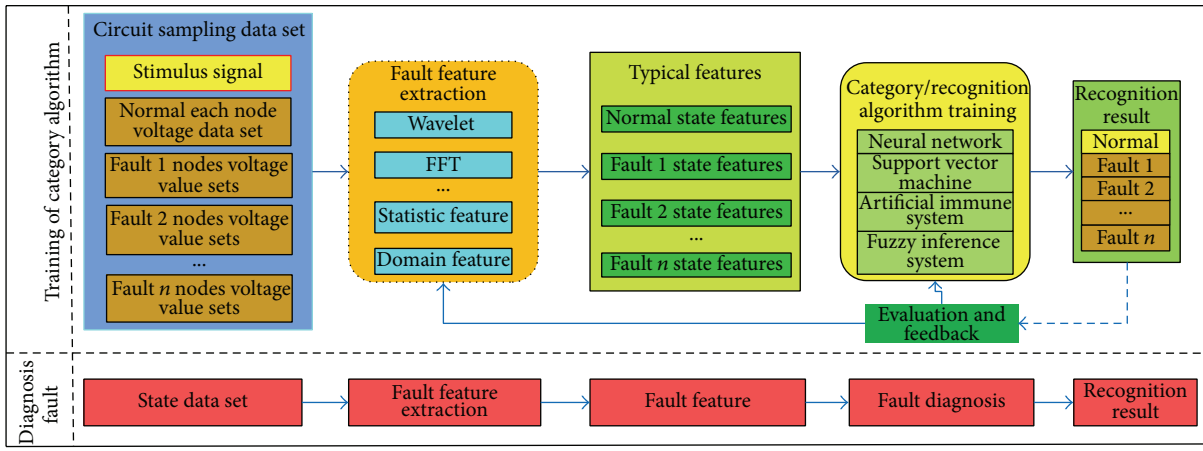

Figure 1: Framework for analog circuit fault diagnosis procedure.

2. PR-Based Fault Diagnosis Approaches for Biquad High-Pass Filter Circuits

If a fault occurs in a certain circuit, there must be some corresponding symptoms, such as the changes in output voltages and/or currents, which contain enormous and untapped potential fault information. Since the transition from operating circuit and faulty circuit is always smooth, one needs to use statistic analysis to establish a threshold. As our focus in this paper is to select wavelet type and optimal features, we choose the same threshold [12] in order to compare the performance fairly. Thus, in this paper by appropriately analyzing the acquired data from the circuit's responses, we would train a classifier for the known faults and then use such classifier to identify any known faults.

Although the faults of analog circuit can be classified into different categories according to different criteria, such as single fault and multiple faults according to the number of the faults, or parametric faults and catastrophic faults according to the deviation from its nominal value, most faults can be detected when a single fault can be identified, since multiple faults can be considered as the superposition of multiple single faults and catastrophic faults can be considered as special soft faults that would remarkably deviate its nominal value. Thus, it is assumed in this paper that only single fault occurred in the CUT.

The framework of PR-based fault diagnosis approaches for biquad high-pass filter analog circuit can be described in Figure 1, consisting of 2 phases: training of classification algorithm and fault diagnosis. Both of these two stages include 5 steps: (i) circuit data acquisition, (ii) fault feature extraction, (iii) typical feature construction, (iv) training (or recognizing) of classification algorithm, and (v) recognition result evaluation and feedback.

The first stage of the framework is circuit data acquisition. In training phase, we would collect all the data used to train classification algorithms, that is, for each type of fault, we would collect its response data for given inputs and train a classifier. In the diagnosis phase, we would use the state response data of CUT with the same input stimuli for classification.

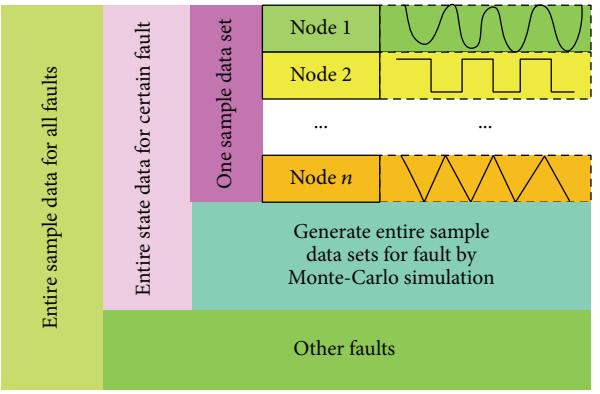

Figure 2: The sampling data sets for biquad high-pass filter circuit under test.

It is well known that a PR-based classification algorithm can identify known faults only. Thus, the generation of node voltage for every potential known faults and the construction of fault dictionary, where the most likely faults are anticipated, are a very critical aspect of the entire approach. One disadvantage of these PR-based fault diagnosing approaches is that it requires a rather large amount of circuit simulations, when one considers all of the various faulty classes for the analog devices with tolerance. The response data of a CUT can be sketched in Figure 2, where the data for different fault classes can be generated for each component using Monte-Carlo techniques and circuit simulation. For example, a simple video amplifier circuit with about twenty components needs about two hours to get only one node's voltage distribution by using SPICE simulator under the computer of Pentium processor level [16].

The collected massive source data would be analyzed and transformed to extract the hidden features in the second stage—fault feature extraction. Due to large amounts of this source data, various algorithms should be skillfully and cleverly designed to extract the features of every fault classes so as to express the most representative characteristics with

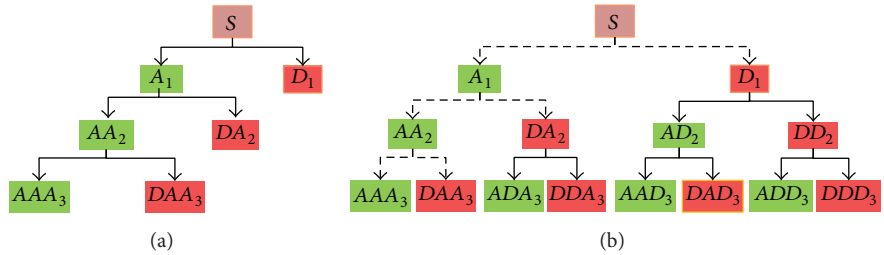

Figure 3: The sketch map of a three-level wavelet tree (a) and wavelet packet decomposition tree (b), where S represents original signal, A represents the low frequency coefficient, and D denotes the high frequency coefficient, and the number represents the decomposition layers.

reduced data and thus decrease the volume of input data as well as increase the efficiency of classifier. As shown in Figure 1, some statistic feature, or domain feature by using FFT or wavelet can be used as preprocessor to extract features. Also in order to use the training knowledge effectively, the feature extraction procedure in diagnosis stage must be exactly the same as that in the training stage.

The third stage is of typical feature construction. One will construct typical fault features with expert's experience or mathematical analysis on the acquired data set.

The fourth stage is training for classification algorithm. Inspired by typical classifier training algorithm such as neural network and fuzzy inference system, this stage takes the fault feature vectors as input and keeps learning the diagnosis knowledge till the training process converges. The learned diagnosis knowledge is integrated as a classifier, which can be used to recognize the same or similar faults in diagnosis stage.

The last stage is the recognition stage. During this phase, the recognition results will be evaluated and possibly used for feedback, and in such case, the parameters of classification algorithm can be adjusted accordingly.

It can be seen from the above process that the extraction and construction of the optimal fault features should be a primary task in this diagnosis process. Next, we will use the wavelet analysis as an effective signal processing technique to investigate the circuit diagnosis problem.

3. Wavelet-Based Feature Extraction for Fault Diagnosis

The wavelet transform (WT) has been proved to be an effective tool for many signal processing applications. It offers simultaneous interpretation of a signal in both time and frequency domain and this will allow local, transient, or intermittent components to be explored. Wavelet transform can be continuous or discrete. The continuous wavelet transform can reveal more details about a signal but its computational time is enormous. For the fault diagnosis application in this paper, however, the goal of using wavelet analysis is to represent a signal efficiently with fewer parameters and less computation time. The discrete wavelet transform (DWT) is more suitable in this case. Next, we will describe WT and DWT briefly.

3.1. Wavelet Transformation. Let $\psi(t) \in L^2(R)$ and its Fourier transform, $\widehat{\Psi}(f)$, satisfy the admissibility condition [31]:

$$C_\Psi = \int_{-\infty}^{\infty} \frac{\left|\widehat{\Psi}(f)\right|^2}{|f|} < \infty, \tag{1}$$

where $\psi(t)$ is a wavelet function and $L^2(R)$ is the space of square integrable complex functions. The wavelet transform of $f(t)$ is defined as [8]

$$\begin{aligned} \mathrm{WT}_f(a,b) &= \langle f(t) \cdot \Psi_{a,b}(t) \rangle \\ &= \frac{1}{\sqrt{a}} \int_0^{\infty} f(t)\, \Psi\left(\frac{t-b}{a}\right) dt, \end{aligned} \tag{2}$$

where $\Psi_{a,b}(t)$ is the scaled and shifted version of the transforming function, called a "mother wavelet" or "base wavelet," which is defined as [1, 32]

$$\Psi_{a,b}(t) = \frac{1}{\sqrt{a}} \Psi\left(\frac{t-b}{a}\right), \tag{3}$$

where $t, a, b \in R$, $a \neq 0$ is continuous variables, a is scale factor of the base wavelet that is responsible for "resolution" analysis, and b is a shift factor that is responsible for location on the time axis. The function $\Psi_{a,b}(t)$ is called the base wavelet (or mother wavelet) and is continuous wavelet when parameters t, a, b change continuously. The discrete wavelet transform is performed by choosing fixed values $a = 2^m$ and $b = n2^m = na$, where m, n are integers. The discrete wavelet analysis can be implemented by the scaling filter, which is a low pass filter related to the scaling function $\varphi(t)$ and the wavelet filter, which is a high-pass filter related to the wavelet function $\Psi(t)$ [33].

In decomposition step, a signal is convolved with a low pass filer L and a high-pass filter H, resulting in two vectors cA_1 and cD_1 (shown in Figure 3(a)). The elements of vector cA_1 are called approximation coefficients and the elements of vector cD_1 are called detail coefficients. The procedure of similar decomposition is repeated on the approximation vector cA_1 and successively on every new approximation vector cA_j, where j is the number of iterations.

3.2. Discrete Wavelet Packet Transform. Wavelet analysis provides a useful tool of signal processing for transient signal analysis, but it results in better time localization in high

frequencies in return for poorer frequency resolution since wavelet transform only implements decomposition on low frequency band of the source data and omits the detail or high frequency.

Because of this problem, wavelet packet analysis was introduced to offer a more efficient decomposition to improve the poor frequency resolution at high frequencies [22]. Daubechies [34] showed that one can numerically obtain wavelet and scaling coefficients at any level, for any node as shown in Figure 3(b). In short, the wavelet packet transform is a generalization of the wavelet transform. The only difference is that the wavelet packet transform decomposes signal not only on the approximations parts, but also on the details parts.

The structure of wavelet decomposition and wavelet packet decomposition (WPD) of a signal S for 3 layers can be shown in Figure 3 [33]. It is observed that the wavelet tree (dashed line) is part of the wavelet packet tree.

3.3. Wavelet-Based Fault Feature Extraction. After a signal is decomposed by a wavelet packet, the wavelet coefficients of each frequency band can be obtained. We define the energy content E_k in each subfrequency band as [35]

$$E_k = \sum_{i=0}^{m} \left(d_i^k\right)^2, \tag{4}$$

where m is the number of the wavelet packet coefficients in each subfrequency band and d_i^k is the wavelet coefficients of k layer. Thus, the high/low frequency coefficients of each layer constitute the energy value of each frequency band.

In most cases, the energy content values can be treated as features to construct a feature vector for faults classification. This energy eigenvector acting as fault feature vector is defined as

$$T = [E_0, E_1, \ldots, E_n]. \tag{5}$$

To eliminate the influence of different absolute value of each component, all these components of the vector should be normalized before they were input into fault diagnosis system. This process is the so-called energized procedure.

By using wavelet transform as preprocessor, the PR-based intelligent fault diagnosis for analog circuit can be shown as Figure 4.

The above wavelet analysis and wavelet-based fault feature extraction are the theoretical basis for our PR-based intelligent fault diagnosis of analog circuit.

3.4. Wavelet-Based Fault Diagnosis Approaches. After wavelet decomposition, a large amount of information embedded in the source data can be converted into energy eigenvector consisting of several coefficients. This reduces the dimension of input data tremendously and improves the efficiency of the classifier greatly. But the following problems should be solved to provide guidelines for the wavelet-based feature extraction and selection.

(1) How to select the suitable mother wavelet?

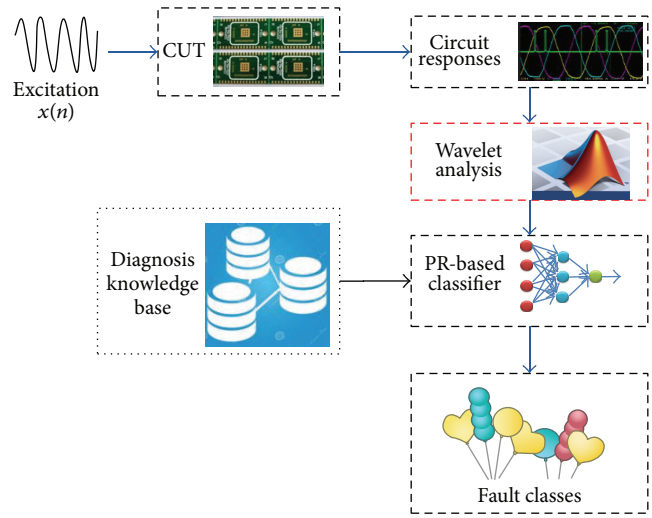

Figure 4: Schematics for intelligent fault classifier using WT as preprocessor.

(2) How many levels of the decomposition are optimal for efficient fault characterizations? Less level decomposition may lead to less information of faults, but more level composition will bring large computational costs as well as extra noise.

(3) How many decomposed coefficients should be chosen?

In order to solve these problems on a biquad high-pass filter circuit, we investigate the criteria of the selection of mother wavelet as well as the various feature construction methods in both decomposition level and wavelet parameters selection by implementing three different groups of comparative experiments.

For completion of this paper, a brief description of typical CSCA (clone algorithm classification algorithm) was presented as below as we will use it as a potential classifier. CSCA is a kind of directed random search technique that mimics the antigen-antibody reaction of the immune system in mammals [36]. In the field of analog circuit fault diagnosis, the antibodies are actually the vectors corresponding to various trained fault class centers, and the antigens are the faults that need to be identified by the classifier. The artificial immune system controls the antibodies evolving to memory antibodies based on negative selection, clone, mutation, clone selection, affinity maturing, and the suppression mechanism.

Fault diagnosis based on CSCA includes two stages: fault knowledge training and fault diagnosis. The first stage takes training samples as initial antibody population and calculates the clustering center (namely, antibody) of each fault class through clone selection algorithm. The diagnosis stage takes testing sample as antigen and regards the clustering center as antibodies and then estimates the status of the input sample through antigen-antibody affinity [37]. The detailed procedures of CSCA are depicted in Pseudocode 1 [38] and can be briefly described as follows.

Input: Ag, MaxGen, N, n, β, d, r
Output: the best antibody in memory cell set M
Initialize the population P (N antibodies Ab_N)
for $t = 1$ to MaxGen
  f = Evaluate(Ab_N, Ag); //evaluate all antibodies in population P
  Ab_N = Selete(f); //select n ($n < N$) antibodies with higher affinity
  Ab_C = Clone(Ab_N, β); //generate clone population P_C
  Ab_M = Mutation(Ab_C); //generate mutated clone population P_M based on P_C
  f^* = Evaluate(Ab_M, Ag); //re-evaluate antibodies in population P_M
  //re-select r best antibodies becoming memory cell set M
  //and replace r worst antibodies in population P with M
  Ab_N = Reselete(Ab_M, f^*, Ab_N);
  Ab_d = Generate(d); //generate d new random antibodies
  Ab_N = Replace(Ab_d, f, Ab_N); //replace d low-affinity antibodies in P with Ab_d
end

Pseudocode 1: Pseudocode of clone selection classification algorithm.

(1) Initialization. The initial population (P) composing N antibodies is randomly generated.

(2) Evaluation. Calculate the affinity of individual antibody **a** as follows:

$$f = \frac{1}{\sum_{i=1}^{k} |a_i - O_i|}, \tag{6}$$

where a_i is component of antibody and O_i is component of the clustering center. Thus, the affinity of antibody with antigen is in the range of (0, 1].

(3) Selection and Cloning. Before generating a new antibody, the n ($n < N$) highest affinity antibodies will be selected firstly. Then these antibodies will be cloned with multiplying factor β. The number of clones reproduced for each individual is proportional to its affinity. After these n best individuals are cloned, a temporary clone population (P_C) is generated.

(4) Mutation. The individuals in the population P_C of the previous step are submitted to a mutation procedure. This can enhance the diversity of antibody population and expand the search space for finding the solution. After mutation, an antibody population (P_M) based on clone population (P_C) is generated.

(5) Reselection. After mutation, the individuals in the population P_M are evaluated again so that the r individuals with higher affinity are chosen to form the memory cell set M.

(6) Replacement. After the above phases are complete, the algorithm proceeds with generation of new individuals. The new randomly generated individuals will be put into population directly so that the lower affinity individuals will be replaced with higher probabilities.

Steps (2)–(6) iteratively proceed until the stopping criterion is reached. The criterion used in this study takes two forms: maximal number of generations and affinity threshold.

4. Experimental Results and Analysis

4.1. CUT and the Experiment Configurations. We use a four-op-amp biquad high-pass filter with components set to their nominal values resulting in a cut-off frequency of 10 kHz, which is the same as in [12] and was shown in Figure 5.

In [12], Aminian et al. adopted Haar wavelet and decomposed the signal into 3 levels (without specified reasons) and selected the approximation coefficient as the fault features. In this paper, our aim is to examine the efficiency of various feature extraction approaches with different wavelet mother selection, decomposing level, and coefficients selection.

In order to compare with existing work fairly, we select the same testing configuration as in [12]. In detail, one collects sufficient data set, including the impulse response of this biquad high-pass filter circuit with resistors and capacitors that allow varying within tolerances of 5% and 10% around the normal class with Gaussian distribution. The used simulator is ORCAD 10.5/pSpice with default Gaussian parameters. When $R1$, $R2$, $R3$, $R4$, $C1$, and $C2$ are 50% higher or lower than the nominal values as shown in Figure 5 and Table 1, we obtain twelve fault classes, named as $R1\uparrow$–$R4\uparrow$, $C1\uparrow$, $C2\uparrow$, $R1\downarrow$–$R4\downarrow$, $C1\downarrow$ and $C2\downarrow$. In this notation, $\uparrow$ and $\downarrow$ stand for high and low, respectively. In order to generate training data for different fault classes, one introduces faulty components in the circuit and varying resistors and capacitors within the standard tolerances of 5% and 10%, respectively. Faulty component values for this circuit are shown in Table 1. All the training data were collected using pSpice [8, 11–14, 16, 28, 39] software, which can simulate the tolerance of analog devices by embedded Monte-Carlo simulation tool. The input pulse is an ideal excitation signal of 5 V peak and 10 μs duration. This stimuli input has rich spectrum information and it can be used to verify different criteria performance for high-pass filters. More importantly, its response can be easily collected with low costs. We select the same stimuli input and responses as in [12], and our aim is different from [12] as we intend to extract the best features based on wavelet analysis. The output voltage data were sampled at point marked as a printer icon (Vplot) in Figure 5 with frequency of 500,000 samples per

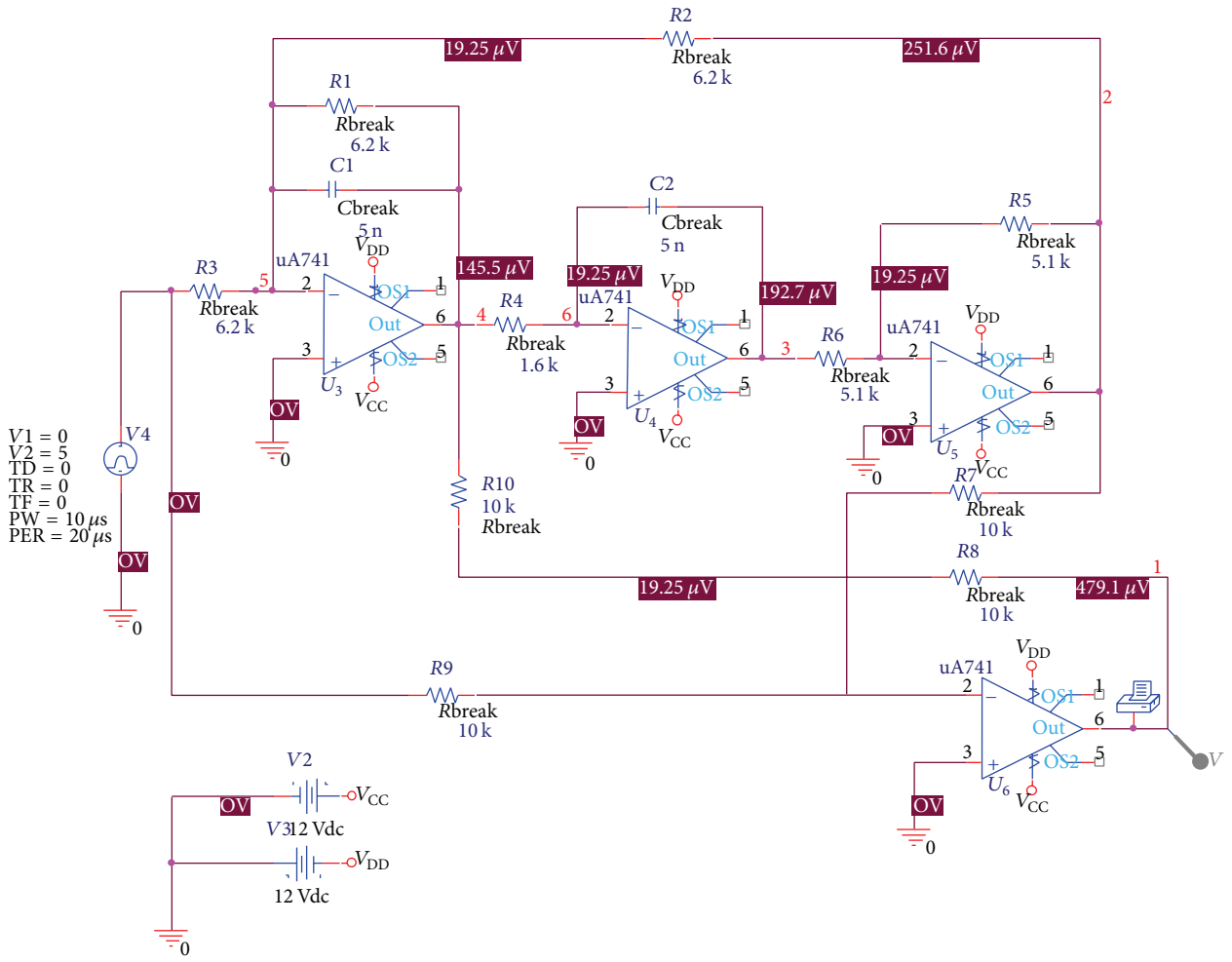

Figure 5: Four-op-amp biquad high-pass filter used in this study (the resistors are in ohms).

second; thus one period of the input pulse training would correspond to 1 ms during which 501 output samples are collected for analysis.

In this study, we have totally 13 classes, including 12 fault classes and 1 normal class. For every fault class, 50 times of Monte-Carlo simulations were carried out to capture the circuit response data, from each of which as much as 1025 output data sets were collected so as to gather enough data for analysis. The analog circuit is a typical high-pass filter and its output with one single impulse input will not oscillate. In the data collection process, we used impulse with peak value 5 V and pulse width 10 μs and periodic 20 μs. The low frequency component is eliminated and the output is a regular signal which seems like an oscillation in Figure 6. The sizes of the training and testing sets for this circuit are 30 (totally 390 groups) and 20 (totally 260 groups) for each fault class, respectively. Therefore, we have 30 multiplied by 1025 samples for each class for training process and 30 multiplied by 1025 samples used for testing process. The average values of the circuit response corresponding to each fault class were shown in Figure 6. The persistent oscillation in this figure is due to periodic impulse response with periodic 20 μs. In fact, there is no oscillation if only one impulse input is given.

Table 1: Fault classes used on the four-op-amp biquad circuit with the specified normal and faulty component values.

Fault class	Nominal	Faulty
$C1\uparrow$	5 nF	10 nF
$C1\downarrow$	5 nF	2.5 nF
$R4\uparrow$	1.6 kΩ	2.5 kΩ
$R4\downarrow$	1.6 kΩ	500 kΩ
$C2\uparrow$	5 nF	15 nF
$C2\downarrow$	5 nF	1.5 nF
$R3\uparrow$	6.2 kΩ	12 kΩ
$R3\downarrow$	6.2 kΩ	2.7 kΩ
$R2\uparrow$	6.2 kΩ	18 kΩ
$R2\downarrow$	6.2 kΩ	2 kΩ
$R1\uparrow$	6.2 kΩ	15 kΩ
$R1\downarrow$	6.2 kΩ	3 kΩ
$R5$, $R6$	5.1 kΩ	—
$R7$, $R8$, $R9$, $R10$	10 kΩ	—

The most important criterion for evaluating the performance of diagnosing methods is their accuracy rate. To

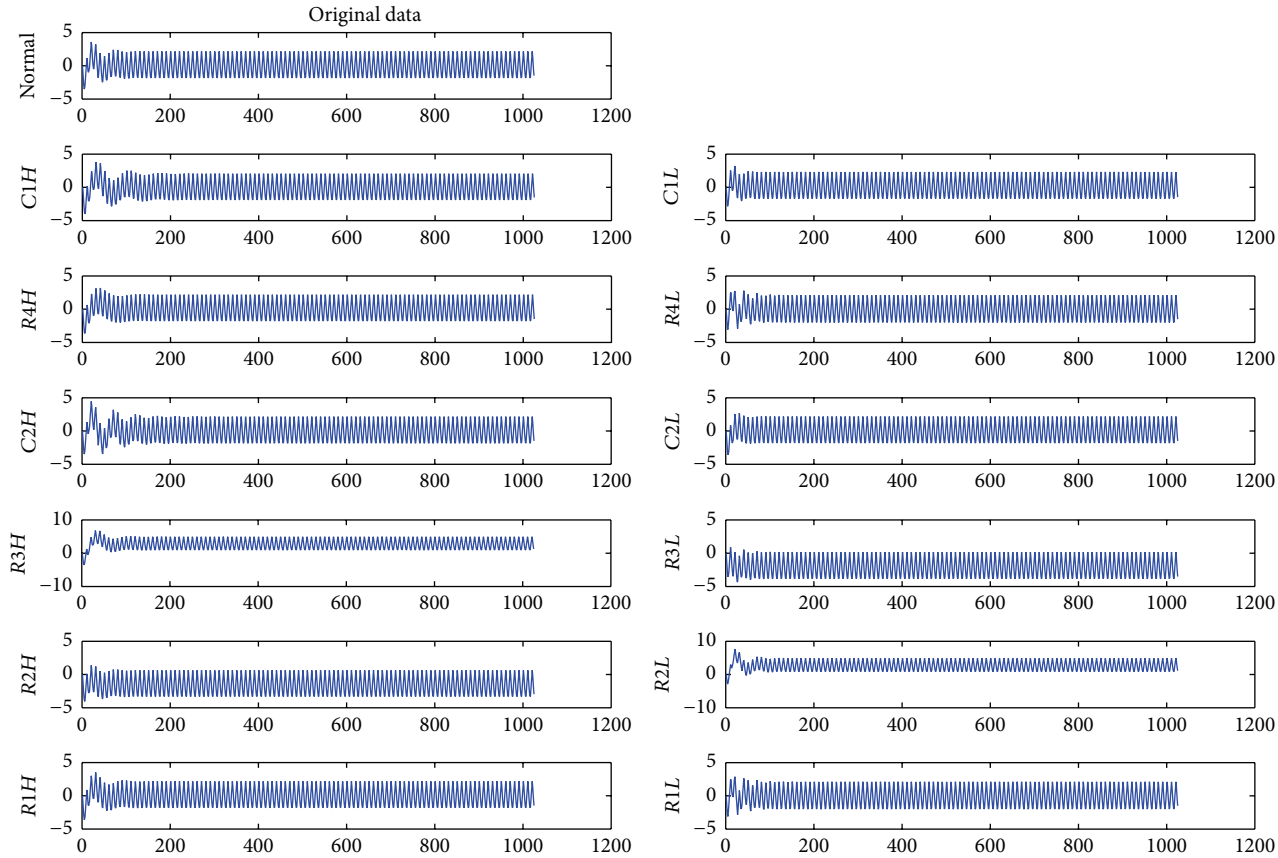

FIGURE 6: Average value of the circuit response corresponding to each fault class, where $C1H$ and $C1L$, equivalent to $C1\uparrow$ and $C1\downarrow$, represent 50% higher or lower than the nominal values of $C1$ and so forth.

compare the performance of different approaches of fault feature extraction, we use the diagnosis rate as an index to indicate the effectiveness of the selected features, and this index is defined to be the ratio between the number of fault classes that were classified correctly and the total number of the entire fault classes. Here, we implement a clonal selection classifier [21, 38] to test the diagnosis rate of each feature extraction approach. As a typical artificial immune system, The clone selection algorithm is known for its fast convergence, escaping from local minima and high self-learning ability [35].

4.2. Selection of the Mother Wavelet. There are several wavelet functions, which can be used for possible candidates of the mother wavelet, so the proper choice of the mother wavelet selected for preprocessing the analog circuit's outputs is crucial for optimal design of the fault diagnostic system. In this section, we have examined five wavelet functions, *Haar, Symlets (sys2), Morlet, Mexican Hat (Mexh), and Meyer*, as possible candidates for the mother wavelet, among which *Haar and sys2* are discrete wavelets, and *Morlet*, *MexH, and Meyer* are continuous wavelets. For the discrete wavelet, we use 5-level decomposition and the first coefficients of approximation from levels 1 to 5 are used as candidate features [12]. In order to keep the same dimension and size of feature vectors, the scales of the continuous wavelet transform, which determine the degree of the wavelet that was compressed or stretched [34], were set as $(1, 2, 3, 4, 5)$. These five sets of wavelet coefficients are then generated and normalized to form a feature vector with 5 components. Classified by the clone selection algorithm, the detailed performance of these mother wavelets is shown in Table 2 and Figure 7. Each row in this table corresponds to one fault class. Different columns then indicate the diagnosing rate that the test data are diagnosed correctly with different mother wavelet.

After analyzing the wavelet coefficients generated by these wavelet functions, the mother wavelet that gave the most distinct features (wavelet coefficients) across fault classes would be selected as the most suitable one for the test circuit to provide the optimal feature.

This group of experiments indicate that, for the four-op-amp biquad high-pass filter, the average diagnosing rate of discrete mother wavelets, that is, $(53.85\% + 52.69\%)/2 = 53.27\%$, is better than continuous mother wavelets, that is, $(56.2\% + 47.69\% + 37.31\%)/3 = 47.06\%$. It is also easy to note that the average diagnosing rate of *Morlet*, 56.2%, is the best among these five wavelets, which was slightly better than that of best discrete mother wavelet, *Haar* with an average diagnosing rate 53.85%. Therefore, the best discrete mother wavelet Haar and the best continuous mother wavelet Morlet were selected for the next group of experiments to study how

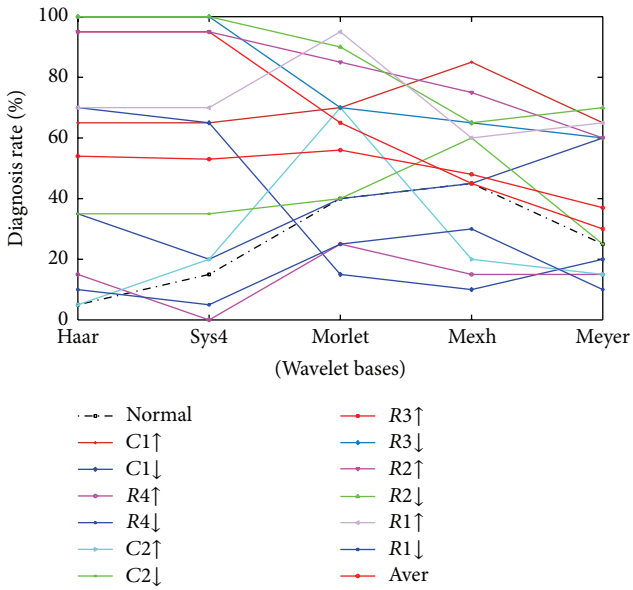

Figure 7: Diagnosis rate using the fault feature constructed by 5 mother wavelets.

Table 2: Diagnosis rate of fault feature constructed by 5 mother wavelets.

Fault classes	Haar	Sys4	Morlet	Mexh	Meyer
Norm	5%	15%	40%	45%	25%
$C1\uparrow$	65%	65%	70%	85%	65%
$C1\downarrow$	70%	65%	15%	10%	20%
$R4\uparrow$	15%	0%	25%	15%	15%
$R4\downarrow$	35%	20%	40%	45%	60%
$C2\uparrow$	5%	20%	70%	20%	15%
$C2\downarrow$	35%	35%	40%	60%	25%
$R3\uparrow$	95%	95%	65%	45%	30%
$R3\downarrow$	100%	100%	70%	65%	25%
$R2\uparrow$	95%	95%	85%	75%	60%
$R2\downarrow$	100%	100%	90%	65%	70%
$R1\uparrow$	70%	70%	95%	60%	65%
$R1\downarrow$	10%	5%	25%	30%	10%
Average	**53.85**%	52.69%	**56.2**%	47.69%	37.31%

the decomposition level and candidate coefficients will be determined.

4.3. Wavelet Decomposition Scales. Given that the mother wavelet had been chosen as in last section, next we should determine how many levels the decomposition of the wavelet should decompose in order to find enough approximation and detailed information. Although five levels had been used for the last group experiments according to [12], it is not a trivial work since the decomposition level is essentially depending on the nature of the signal and the application. Since the fault features extracted by *Haar and Morlet* wavelet show the best performance in the previous experiments, different decomposition levels were compared to reveal the tradeoff between efficiency of diagnosis and computational costs. The clonal selection classifier is used again to calculate the diagnosing rate for each group of experiments.

Table 3: Diagnosis rate of fault feature by Haar wavelet at five different decomposition levels.

Fault classes	1 level	3 levels	5 levels	7 levels	9 levels
Norm	15%	30%	70%	70%	70%
$C1\uparrow$	95%	75%	90%	90%	90%
$C1\downarrow$	100%	80%	85%	85%	85%
$R4\uparrow$	0%	15%	20%	30%	30%
$R4\downarrow$	30%	45%	50%	50%	50%
$C2\uparrow$	25%	45%	45%	55%	55%
$C2\downarrow$	45%	55%	70%	70%	70%
$R3\uparrow$	95%	85%	95%	100%	100%
$R3\downarrow$	100%	85%	100%	100%	100%
$R2\uparrow$	100%	100%	100%	100%	100%
$R2\downarrow$	80%	85%	95%	95%	95%
$R1\uparrow$	35%	75%	95%	95%	95%
$R1\downarrow$	10%	15%	30%	45%	45%
Average	56.2%	60.8%	72.7%	**75.8**%	75.8%
Increment	/	4.6%	11.9%	3.1%	0

The *Haar* wavelet is investigated first. The obtained data is decomposed to 1, 3, 5, 7, and 9 levels, respectively, and then all coefficients of each level are assembled as the fault features. Next, these coefficients were energized as indicated in formula (4), normalized, and input into the clonal selection classifier to determine the fault class. Table 3 and Figure 8 listed the diagnosing rate of these 5 groups.

Our results clearly indicate that the diagnosing rate is increasing with more levels of the wavelet decomposition till 7 levels as there is no improvement when the decomposition level is up to the 9 levels from 7 levels.

Then the effectiveness of different decomposition scale for the Morlet wavelet is investigated. The groups done in Section 4.2 were named group A, and we have transformed the source data in more detailed scales with group B = [1 3 5 7 9 11 13 15 17 19] (totally 10), group C = [1 : 2 : 29] (totally 15), group D = [1 : 2 : 39] (totally 20), group E = [1 : 2 : 59] (totally 30), group F = [1 : 2 : 79] (totally 40), group G = [1 : 2 : 99] (totally 50), and group H = [1 : 2 : 199] (totally 100), respectively. And also the obtained coefficients of each scale are assembled as the fault feature and then were energized, normalized, and presented to the clonal selection classifier to examine the efficiency of diagnosis. The results of these experiments are presented in Table 4 and Figure 9.

Our results indicate that the overall accuracy of diagnosing system is improved continuously with the increasing of the decomposition scales until it reached the upper bound that was determined by the circuit's outputs, but the increment has declined when the level of scales was greater than E groups, which indicates that this represents the possible best decomposition level.

It is important to note that the search for candidate features does not need to be exhaustive. All we required is to select a few candidate features that can be distinguished among fault classes. Group H shows that even the scale

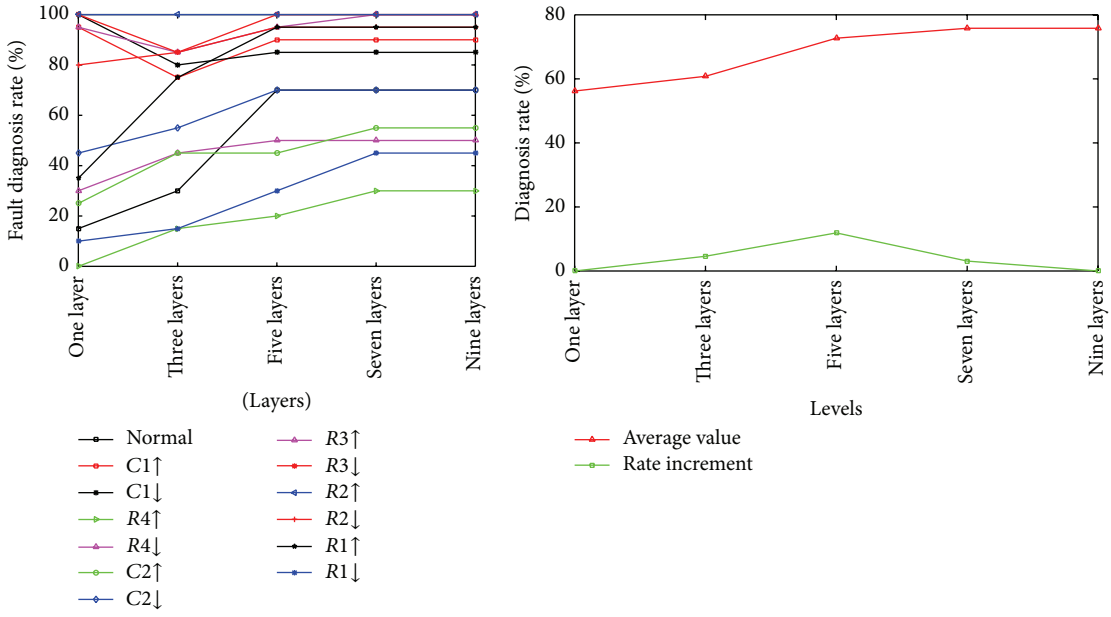

(a) Diagnosis rate of 13 fault classes for five different wavelet layers

(b) Averages diagnosis rate and the increment of different levels

Figure 8: Diagnosis rate of fault feature by Haar wavelet at five different decomposition levels.

Table 4: Diagnosis rate of fault feature by Morelet wavelet at eight different decomposition scales.

Fault classes	A (5)	B (11)	C (15)	D (20)	E (30)	F (40)	G (50)	H (100)
Norm	40%	60%	90%	95%	95%	95%	95%	95%
$C1\uparrow$	70%	100%	100%	100%	100%	100%	100%	100%
$C1\downarrow$	15%	35%	40%	40%	50%	50%	50%	65%
$R4\uparrow$	25%	25%	25%	50%	90%	85%	95%	95%
$R4\downarrow$	40%	30%	40%	40%	40%	40%	40%	40%
$C2\uparrow$	70%	55%	65%	75%	80%	85%	85%	85%
$C2\downarrow$	40%	70%	70%	70%	70%	70%	70%	70%
$R3\uparrow$	65%	100%	100%	100%	100%	100%	100%	100%
$R3\downarrow$	70%	85%	95%	95%	100%	100%	100%	100%
$R2\uparrow$	85%	95%	100%	100%	100%	100%	100%	100%
$R2\downarrow$	90%	85%	100%	100%	100%	100%	100%	100%
$R1\uparrow$	95%	90%	90%	100%	100%	100%	100%	100%
$R1\downarrow$	25%	25%	55%	70%	95%	100%	100%	100%
Average	56.2%	65.8%	74.6%	79.6%	86.2%	86.5%	87.3%	88.5%
Increment	/	9.6%	8.8%	5%	6.6%	0.3%	0.8%	1.2%

was enlarged to 2 times group G, from 50 to 100, and the diagnosing rate has been improved merely 1.2%. In consideration of the balance between the diagnosing performance and computational cost, it offers superior efficiency and computing time and is the most suitable decomposition level for fault diagnostic problems when the decomposition scale runs up to 50 (group G), where 12 out of 13 fault classes reach their peak rates.

4.4. Selection of Candidate Coefficients. Based on analysis in [12], approximation coefficients are appropriate features for this type of analog circuit fault diagnosis since they represent the low frequency contents or basic structure of a signal. One should also note that the details coefficients of wavelet decomposition that capture the high frequency contents of a signal are inseparable part of the source data. In fact, the wavelet coefficients associated with all levels then form all the possible features for our study. The selection of the candidate coefficients as features also plays an important role when the mother wavelet and decomposition scale have been decided as investigated in last two sections.

In this part, the fault features were constructed by three different approaches by selecting different approximation and detail coefficients generated by 7-level Haar wavelet packet decomposition. These fault features are then energized, normalized, and input into the clonal selection classifier.

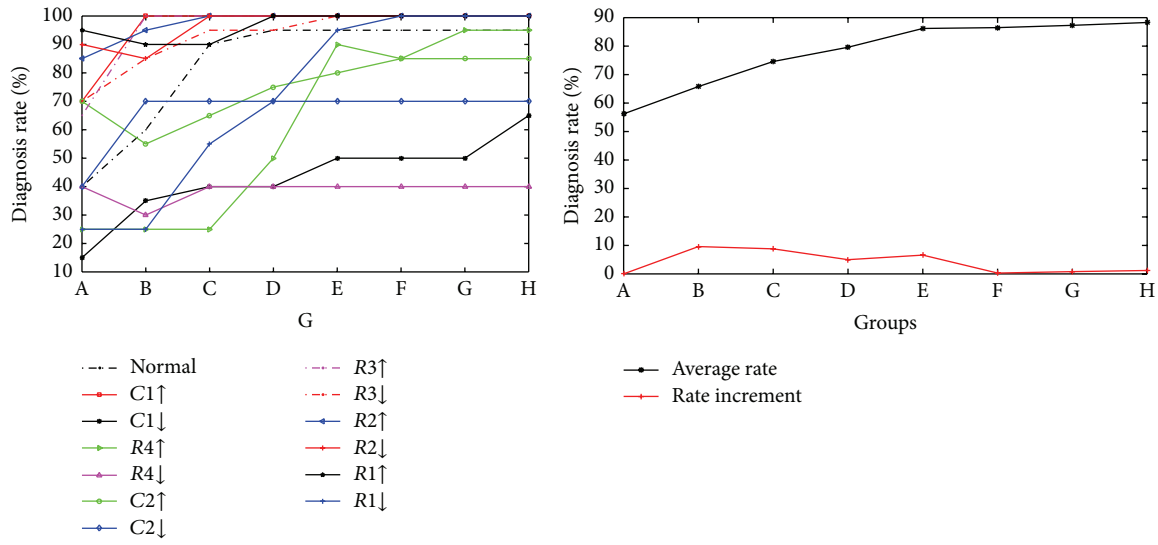

(a) Diagnosis rate of 13 fault classes

(b) Averages diagnosis rate and rate increments

Figure 9: Diagnosis rate of fault feature by Morlet wavelet at 8 different decomposition scales.

Fault features group A only takes the first approximation coefficients of the 7th level, and in group B, the first coefficients of approximation in levels 1 through 5 are used. In group C, however, all the approximation and detail coefficients from level 1 to level 7 are taken into consideration. In addition, through the observation of the sample data, we noted that every fault class has its own unstable period last about 12 cycles. To investigate their influences on the feature vector, we then removed these unsteady data of each fault mode and made another group D, whose feature construction method is kept the same as that of group C. Figure 10 and Table 5 show the effectiveness of these features.

Observation of the average diagnosing rate in the second column (54.6%) and first column (38.5%) of Table 5 reveals that features extracted from level 1 to level 7 contain more useful information for fault identification. The comparative result between the average diagnosing rate in third column (75.8%) and the second column (54.6%) clearly shows the advantage of detail coefficients of WPD. The fact that average diagnosing rate of group D (67.7%) is lower than C (75.8%) indicates that the selection of response data has significant relationship with the diagnosis accuracy, which will be investigated in future work.

In summary, we can conclude the contributions of our paper as below.

(1) The mother wavelets of *Haar and Morlet* demonstrated the best performance among the selected five discrete mother wavelets and continuous mother wavelets.

(2) The diagnosis accuracy was improved with the increasing of decomposition level of the wavelet until the best diagnosing rate was achieved. And also the best decomposing level can be computed for *both Haar and Morlet wavelet* based on identification rate.

Table 5: Diagnosis rate of fault feature by different coefficients under a 7-level Haar wavelet packet decomposition.

Fault classes	Group A	Group B	Group C	Group D
Norm	0%	10%	70%	60%
$C1\uparrow$	35%	55%	90%	95%
$C1\downarrow$	0%	65%	85%	85%
$R4\uparrow$	5%	15%	30%	15%
$R4\downarrow$	0%	45%	50%	40%
$C2\uparrow$	65%	0%	55%	60%
$C2\downarrow$	5%	25%	70%	65%
$R3\uparrow$	95%	95%	100%	95%
$R3\downarrow$	100%	100%	100%	100%
$R2\uparrow$	95%	100%	100%	100%
$R2\downarrow$	100%	85%	95%	95%
$R1\uparrow$	0%	15%	95%	70%
$R1\downarrow$	0%	10%	45%	0%
Average	38.5%	54.6%	75.8%	67.7%

(3) Either approximation coefficients or detail coefficients of WPD on the specified circuit response data contain useful information for fault diagnosis.

5. Conclusions

In this paper, we investigate the selection of mother wavelet, decomposition level, and feature extraction for fault diagnosis of the biquad high-pass filter circuit based on input and output response data. For these purposes, three groups of experiments were carried out and some interesting conclusions have been obtained. We believe the proposed approach can be used to other analog circuits if the response data with fault requirements are available.

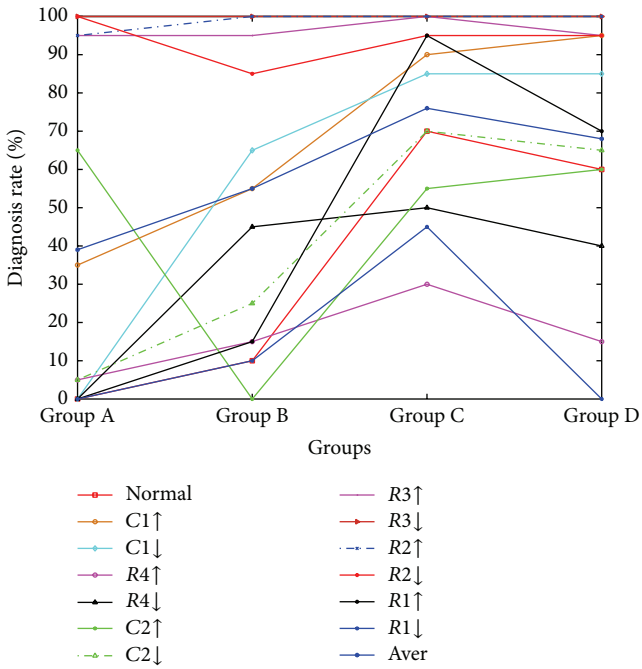

Figure 10: Diagnosis rate of fault feature constructed by different coefficients under a 7-level Haar wavelet packet decomposition.

The proposed approach and its demonstrative results in this paper would motivate us to do more research in this area from both data response point of view and theoretical analysis. First, from data-drive point of view, we can conduct similar study on some other typical analog circuits including high frequency or amplifiers. Another future direction is to investigate the selection of different input stimuli. Of course, we need to establish the faulty detection tolerance threshold via data statistic analysis.

Second, from theoretical point of view, one important question is to investigate theoretical difference between the selected mother wavelet in this paper and other mother wavelets and give a justifiable interpretation for the selection in this paper. Also how the selected coefficients are related to the circuit behaviour in time or frequency domain deserves theoretical analysis.

Competing Interests

The authors declare that they have no competing interests.

Acknowledgments

This work was supported by the Cultivation Program for Young Talents of Beijing Municipal Institutions under Grant no. CIT&TCD201504002. The authors wish to acknowledge some valuable comments from Drs. Yang Yang, Peng Mao, and Mr. Jiancheng Feng in the preparation and revision of this paper.

References

[1] L. Chruszczyk, "Wavelet transform in fault diagnosis of analogue electronic circuits," in *Advances in Wavelet Theory and Their Applications in Engineering, Physics and Technology*, D. D. Baleanu, Ed., InTech, 2012.

[2] F. Li and P.-Y. Woo, "Fault detection for linear analog IC—the method of short-circuit admittance parameters," *IEEE Transactions on Circuits and Systems I: Fundamental Theory and Applications*, vol. 49, no. 1, pp. 105–108, 2002.

[3] M. Catelani and A. Fort, "Soft fault detection and isolation in analog circuits: some results and a comparison between a fuzzy approach and radial basis function networks," *IEEE Transactions on Instrumentation and Measurement*, vol. 51, no. 2, pp. 196–202, 2002.

[4] S. Yang, *Analog System Fault Diagnosis and Reliability Design*, Tsinghua University Press, Beijing, China, 2001.

[5] R. S. Berkowitz, "Conditions for network-element-value solvability," *IRE Transactions on Circuit Theory*, vol. 9, no. 1, pp. 24–29, 1962.

[6] N. Navid and J. Willson, "A theory and an algorithm for analog circuit fault diagnosis," *IEEE Transactions on Circuits and Systems*, vol. 26, no. 7, pp. 440–457, 1979.

[7] J. W. Bandler and A. E. Salama, "Fault diagnosis of analog circuits," *Proceedings of the IEEE*, vol. 73, no. 8, pp. 1279–1325, 1985.

[8] Y. Tan, Y. He, C. Cui, and G. Qiu, "A novel method for analog fault diagnosis based on neural networks and genetic algorithms," *IEEE Transactions on Instrumentation and Measurement*, vol. 57, no. 11, pp. 2631–2639, 2008.

[9] Y.-Y. Hong and W.-S. Huang, "Locating high-impedance fault section in electric power systems using wavelet transform, k-means, genetic algorithms, and support vector machine," *Mathematical Problems in Engineering*, vol. 2015, Article ID 823720, 9 pages, 2015.

[10] R. Spina and S. Upadhyaya, "Linear circuit fault diagnosis using neuromorphic analyzers," *IEEE Transactions on Circuits and Systems II: Analog and Digital Signal Processing*, vol. 44, no. 3, pp. 188–196, 1997.

[11] M. Aminian and F. Aminian, "Neural-network based analog-circuit fault diagnosis using wavelet transform as preprocessor," *IEEE Transactions on Circuits and Systems II: Analog and Digital Signal Processing*, vol. 47, no. 2, pp. 151–156, 2000.

[12] F. Aminian, M. Aminian, and H. W. Collins Jr., "Analog fault diagnosis of actual circuits using neural networks," *IEEE Transactions on Instrumentation and Measurement*, vol. 51, no. 3, pp. 544–550, 2002.

[13] M. Aminian and F. Aminian, "A modular fault-diagnostic system for analog electronic circuits using neural networks with wavelet transform as a preprocessor," *IEEE Transactions on Instrumentation and Measurement*, vol. 56, no. 5, pp. 1546–1554, 2007.

[14] L. Yuan, Y. He, J. Huang, and Y. Sun, "A new neural-network-based fault diagnosis approach for analog circuits by using kurtosis and entropy as a preprocessor," *IEEE Transactions on Instrumentation and Measurement*, vol. 59, no. 3, pp. 586–595, 2010.

[15] P. Li, Y. Chai, M. Cen, Y. Qiu, and K. Zhang, "Multiple fault diagnosis of analog circuit using quantum hopfield neural network," in *Proceedings of the 25th Chinese Control and Decision Conference (CCDC '13)*, pp. 4238–4243, Guiyang, China, May 2013.

[16] P. Wang and S. Yang, "A new diagnosis approach for handling tolerance in analog and mixed-signal circuits by using fuzzy math," *IEEE Transactions on Circuits and Systems I: Regular Papers*, vol. 52, no. 10, pp. 2118–2127, 2005.

[17] B. H. Ulutas and S. Kulturel-Konak, "A review of clonal selection algorithm and its applications," *Artificial Intelligence Review*, vol. 36, no. 2, pp. 117–138, 2011.

[18] D. Dasgupta, "Advances in artificial immune systems," *IEEE Computational Intelligence Magazine*, vol. 1, no. 4, pp. 40–43, 2006.

[19] I. Aydin, M. Karakose, and E. Akin, "An adaptive artificial immune system for fault classification," *Journal of Intelligent Manufacturing*, vol. 23, no. 5, pp. 1489–1499, 2012.

[20] C. He, J. Li, and G. Vachtsevanos, "Prognostics and health management of an automated machining process," *Mathematical Problems in Engineering*, vol. 2015, Article ID 651841, 10 pages, 2015.

[21] L. N. De Castro and F. J. Von Zuben, "Learning and optimization using the clonal selection principle," *IEEE Transactions on Evolutionary Computation*, vol. 6, no. 3, pp. 239–251, 2002.

[22] R. R. Coifman and M. V. Wickerhauser, "Entropy-based algorithms for best basis selection," *IEEE Transactions on Information Theory*, vol. 38, no. 2, pp. 713–718, 1992.

[23] H. Yuan, G. Chen, and Y. Xie, "Feature evaluation and extraction based on neural network in analog circuit fault diagnosis," *Journal of Systems Engineering and Electronics*, vol. 18, no. 2, pp. 434–437, 2007.

[24] X. He, H. Wang, J. Lu, and W. Jiang, "Analog circuit fault diagnosis method based on preferred wavelet packet and ELM," *Chinese Journal of Scientific Instrument*, vol. 34, no. 11, pp. 2614–2619, 2013.

[25] J. Sun and C. Wang, "Analog circuit fault diagnosis based on mRMR and optimized SVM," *Chinese Journal of Scientific Instrument*, vol. 34, no. 1, pp. 221–226, 2013.

[26] K. Guo, S. Wang, and J. Song, "Analog circuit fault diagnosis based on wavelet kernel support vector machine," in *Proceedings of the International Conference on Information Technology and Applications (ITA '13)*, pp. 395–399, Chengdu, China, November 2013.

[27] A.-N. Wang, J.-F. Liu, W.-J. Yuan, and H. Li, "Algorithms comparison of feature extraction and multi-class classification for fault diagnosis of analog circuit," in *Proceedings of the International Conference on Wavelet Analysis And Pattern Recognition*, vol. 1–4, pp. 566–572, Beijing, China, November 2007.

[28] Y. He, Y. Tan, and Y. Sun, "Wavelet neural network approach for fault diagnosis of analogue circuits," *IEE Proceedings—Circuits, Devices and Systems*, vol. 151, no. 4, pp. 379–384, 2004.

[29] P. Li, J. Jiang, B. Qiu, and Z. Liang, "A fault diagnosis method of analog circuit using energy calculation and Hopfield neural network," *Journal of Chongqing University (Natural Science Edition)*, vol. 37, no. 7, pp. 136–146, 2014.

[30] H. Liu, G. Chen, S. Jiang, and G. Song, "A survey of feature extraction approaches in analog circuit fault diagnosis," in *Proceedings of the Pacific-Asia Workshop on Computational Intelligence and Industrial Application (PACIIA '08)*, Y. Zhang, H. Tan, and Q. Luo, Eds., vol. 1–3, pp. 1635–1639, Wuhan, China, December 2008.

[31] G. Liu, J. Long, L. Yang, Z. Su, D. Yao, and X. Zhong, "Detection and diagnosis of urban rail vehicle auxiliary inverter using wavelet packet and RBF neural network," *Journal of Intelligent Learning Systems and Applications*, vol. 5, no. 4, pp. 211–215, 2013.

[32] C. S. Tyagi, "A comparative study of SVM classifiers and artificial neural networks application for rolling element bearing fault diagnosis using wavelet transform preprocessing," *International Journal of Mechanical, Aerospace, Industrial, Mechatronic and Manufacturing Engineering*, vol. 2, no. 7, pp. 904–912, 2008.

[33] N. G. Nikolaou and I. A. Antoniadis, "Application of wavelet packets in bearing fault diagnosis," in *Proceedings of the 5th WSES International Conference on Circuits, Systems, Communications and Computers (CSCC '01)*, Rethymno, Greece, 2001.

[34] I. Daubechies, *Ten Lectures on Wavelets*, Conference Board in Mathematical Science, Society for Industrial and Applied Mathematics, Philadelphia, Pa, USA, 1992.

[35] L.-Y. Zhao, L. Wang, and R.-Q. Yan, "Rolling bearing fault diagnosis based on wavelet packet decomposition and multiscale permutation entropy," *Entropy*, vol. 17, no. 9, pp. 6447–6461, 2015.

[36] W. J. Tian, Y. Geng, J. C. Liu, and L. Ai, "Support vector regression and immune clone selection algorithm for intelligent electronic circuit fault diagnosis," in *Proceedings of the Pacific-Asia Conference on Circuits, Communications and System (PACCS '09)*, pp. 297–300, IEEE Computer Society, Chengdu, China, May 2009.

[37] Y. Li, J. Chen, and Z. Pang, "Application of immune clustering algorithm to analog circuit fault diagnosis," in *Proceedings of the International Conference on Transportation, Mechanical, and Electrical Engineering (TMEE '11)*, pp. 1743–1746, IEEE Computer Society, Changchun, China, December 2011.

[38] Z. Gan, M.-B. Zhao, and T. W. S. Chow, "Induction machine fault detection using clone selection programming," *Expert Systems with Applications*, vol. 36, no. 4, pp. 8000–8012, 2009.

[39] Y. He, T. Yanghong, and S. Yichuang, "Fault diagnosis of analog circuits based on wavelet packets," in *Proceedings of the IEEE Region 10 Conference (TENCON '04)*, November 2004.